THE JOURNAL OF BIOLOGICAL CHEMISTRY VOL. 286, NO. 37, pp. 32259–32267, September 16, 2011

Allyl Isothiocyanate Arrests Cancer Cells in Mitosis, and Mitotic Arrest in Turn Leads to Apoptosis via Bcl-2 Protein Phosphorylation*[S]

Received for publication, June 30, 2011, and in revised form, July 16, 2011 Published, JBC Papers in Press, July 21, 2011, DOI 10.1074/jbc.M111.278127

Feng Geng[‡], Li Tang[‡], Yun Li[‡], Lu Yang[‡], Kyoung-Soo Choi[§], A. Latif Kazim[§], and Yuesheng Zhang[‡1]

From the Departments of [‡]Cancer Prevention and Control and [§]Cell Stress Biology, Roswell Park Cancer Institute, Buffalo, New York 14263

Allyl isothiocyanate (AITC) occurs in many commonly consumed cruciferous vegetables and exhibits significant anti-cancer activities. Available data suggest that it is particularly promising for bladder cancer prevention and/or treatment. Here, we show that AITC arrests human bladder cancer cells in mitosis and also induces apoptosis. Mitotic arrest by AITC was associated with increased ubiquitination and degradation of α- and β-tubulin. AITC directly binds to multiple cysteine residues of the tubulins. AITC induced mitochondrion-mediated apoptosis, as shown by cytochrome *c* release from mitochondria to cytoplasm, activation of caspase-9 and caspase-3, and formation of TUNEL-positive cells. Inhibition of caspase-9 blocked AITC-induced apoptosis. Moreover, we found that apoptosis induction by AITC depended entirely on mitotic arrest and was mediated via Bcl-2 phosphorylation at Ser-70. Pre-arresting cells in G_1 phase by hydroxyurea abrogated both AITC-induced mitotic arrest and Bcl-2 phosphorylation. Overexpression of a Bcl-2 mutant prevented AITC from inducing apoptosis. We further showed that AITC-induced Bcl-2 phosphorylation was caused by c-Jun N-terminal kinase (JNK), and AITC activates JNK. Taken together, this study has revealed a novel anticancer mechanism of a phytochemical that is commonly present in human diet.

Allyl isothiocyanate (AITC)[2] is a naturally occurring compound that possesses both antimicrobial and anticancer activities. Many commonly consumed cruciferous vegetables are rich sources of AITC, such as mustard, horseradish, wasabi, and cabbage. Its bactericidal and fungicidal activities were demonstrated against a variety of pathogens, and its anticancer activities were shown in both cultured cancer cell lines and animal tumor models (1). Bioavailability of AITC is extremely high; nearly 90% of orally administered AITC is absorbed (1). Although available evidence indicates that the anticancer activity of AITC is neither cell- nor tissue-specific, we have recently shown that AITC is selectively delivered to bladder tissue through urinary excretion and potently inhibits cancer development and muscle invasion in an orthotopic rat bladder cancer model (2). Moreover, an AITC-rich mustard seed powder also strongly inhibited bladder cancer development and muscle invasion *in vivo* (3). Thus, AITC is highly promising for bladder cancer prevention and/or treatment. These results are also consistent with epidemiological studies showing an inverse association between consumption of cruciferous vegetables and bladder cancer risk (4, 5). In light of these findings, this study focuses on human bladder cancer cells.

Previous studies have shown that AITC causes cell cycle arrest and apoptosis in cancer cell lines of different tissue origins *in vitro* and in several tumor xenograft models *in vivo*, and it modulates many genes and proteins involved in cancer cell survival and proliferation (1). In our recent studies, both AITC and the AITC-rich mustard seed powder mentioned above arrested bladder cancer cells in G_2/M phases and activated caspase-3 in bladder cancer cells *in vitro* and in bladder tumors *in vivo* (2, 3). However, it has not been determined whether AITC arrests cancer cells in both the G_2 phase and M phase or only in one of the two phases. It is not known whether cell cycle arrest and apoptosis are linked to each other in AITC-treated cells. Answers to these questions are important for further development of this interesting agent against cancer. In this study, we show that AITC arrests bladder cancer cells exclusively in mitosis and targets two key proteins involved in mitosis. We also demonstrate that AITC induces mitochondrion-mediated apoptosis, but the apoptosis induction results entirely from mitotic arrest and that Bcl-2 phosphorylation by c-Jun N-terminal kinase (JNK) bridges mitotic arrest to apoptosis in response to AITC. Our study shows that AITC-treated cells die by mitotic catastrophe via Bcl-2 phosphorylation.

EXPERIMENTAL PROCEDURES

Cells and Chemicals—Three human bladder cancer cell lines, all derived from invasive transitional cell carcinomas, were used, including UM-UC-3 cells, UM-UC-6 cells, and T24 cells. Their sources and culture conditions have been described previously (6, 7). AITC, benzyl isothiocyanate (BITC), SP600125, and hydroxyurea (HU) were purchased from Sigma. Z-LEHD-FMK, rhodamine 123, MG-132, and JNK inhibitor XI (BI-87G3) were purchased from R & D Systems, Molecular Probes, EMD Millipore, and EMD/Calbiochem, respectively. HU was

* This work was supported, in whole or in part, by National Institutes of Health Grant R01CA124627.

[S] The on-line version of this article (available at http://www.jbc.org) contains supplemental Figs. S1–S3.

[1] To whom correspondence should be addressed: Elm and Carlton St., Basic Science 711, Buffalo, NY 14263. Fax: 716-845-1144; E-mail: yuesheng.zhang@roswellpark.org.

[2] The abbreviations used are: AITC, allyl isothiocyanate; BITC, benzyl isothiocyanate; Cyt *c*, cytochrome c; HU, hydroxyurea; PARP, poly(ADP-ribose) polymerase; Ub, ubiquitin; JNK, c-Jun N-terminal kinase; IP, immunoprecipitation.

dissolved in water; other agents were dissolved in acetonitrile or DMSO; solvent concentrations in culture medium was ≤0.1% (v/v). Antibodies specific for Bcl-2, p-Bcl-2 (Ser(P)-87), His tag (His-probe H3), cytochrome *c* (Cyt *c*), lamin B1, α-tubulin (for IP), β-tubulin (for IP), and γ-tubulin were purchased from Santa Cruz Biotechnology. Antibodies specific for Bad, Bak, Bax, Bcl-xl, Bid, p-Bcl-2 (Ser(P)-70), β-tubulin (for Western blotting), caspase-3, cleaved caspase-3, caspase-9, cleaved caspase-9, poly(ADP-ribose) polymerase (PARP), cleaved PARP, JNK, JNK1, JNK2, JNK3, p-JNK (Thr-183/Tyr-185), and voltage-dependent anion channel were purchased from Cell Signaling Technology. Antibodies specific for α-tubulin (for Western blotting), matrix metallopeptidase 9 (MMP-9), and glyceraldehyde 3-phosphate dehydrogenase (GAPDH) were purchased from EMD/Calbiochem and Millipore, respectively.

Transient Gene Transfection—Cells were seeded in 10-cm dishes (1.5×10^6 cells/dish with 10 ml of medium) for 24 h and then transfected with pSFFV-neo (empty vector), pSFFV-HA-hBcl-2Δ (deletion of the loop domain of human Bcl-2 or amino acid residues 32–80), or pMT107-His-Ub (6× polyhistidine-tagged ubiquitin expression plasmid), 6–12 μg of DNA/dish and using FuGENE HD transfection reagent (Roche Applied Science); after 24 h, cells were treated with solvent or AITC for a desired time and then harvested for analysis.

Cell Cycle Analysis, Measurement of Mitochondrial Trans-membrane Potential, and TdT-mediated dUTP-biotin Nick End Labeling (TUNEL) Assay—Cells were seeded in 10-cm dishes ($1.5–3 \times 10^6$ cells/dish with 10 ml of medium) for 24 h and then subjected to various treatments. At the end of each treatment, cells were processed for determination of cell cycle progression by flow cytometry as described previously (6). For measurement of mitochondrial trans-membrane potential, cells were first treated with vehicle or AITC and then trypsinized, washed, and centrifuged. Each cell pellet was resuspended in fresh medium at 5×10^5 cells/ml and then incubated with rhodamine 123 at 10 μg/ml for 30 min at 37 °C. The cells were then washed twice, resuspended in an equal volume of fresh medium, and measured by flow cytometry (1×10^4 cells/sample). For TUNEL assay, cells after treatment with AITC or solvent were processed using the MEBSTAIN® apoptosis kit (MBL International), following the manufacturer's instruction, and finally measured for TUNEL-positive cells by flow cytometry.

Western Blot Analysis—Cells harvested after treatment with solvent or AITC were washed with ice-cold PBS and suspended in 1× cell lysis buffer (Cell Signaling), supplemented with 2 mM phenylmethanesulfonyl fluoride (PMSF) and a proteinase inhibitor mixture (Roche Applied Science). Cell lysis was enhanced by sonication. Mitochondria and cytosols were prepared based on a published protocol (8) with a minor modification. Briefly, $\sim 2 \times 10^7$ cells were washed with ice-cold PBS, placed on ice for 10 min, and then suspended in 0.75 ml of an isotonic homogenization buffer (25 mM sucrose, 10 mM KCl, 1.5 mM $MgCl_2$, 1 mM NaEDTA, 1 mM NaEGTA, 1 mM dithiothreitol, 0.1 mM PMSF, 10 mM Tris-HCl, pH 7.4, and a proteinase inhibitor mixture from Roche Applied Science). The cells were stroked in a Dounce homogenizer. The homogenates were cleared by low speed centrifugation, and the supernatant was centrifuged at 12,000 × *g* for 20 min at 4 °C. The resultant supernatant was collected as cytosols, and the pellet containing mitochondria was washed three times with the homogenization buffer containing 0.01% Nonidet P-40 and then suspended in 1× cell lysis buffer (Cell Signaling). Protein contents were measured using a bicinchoninic acid assay kit (Pierce). The samples (20–40 μg each) were resolved by SDS-PAGE (8–12%, unless specified otherwise), which was followed by blotting to polyvinylidene fluoride membranes. The membranes were then probed by specific antibodies and the bands were visualized using the SuperSignal West Pico chemiluminescence kit (Thermo Scientific) or Amersham Biosciences ECL Plus kit (GE Healthcare).

Immunoprecipitation—Cells were lysed in 5 volumes of lysis buffer (10 mM Tris, pH 8.0, 0.25 mM EDTA, and 1% SDS), boiled immediately for 5 min, and then mixed with 10 volume of IP buffer (10 mM Tris, pH 8.0, 150 mM NaCl, 0.1 mM EDTA, and 0.5% Tween 20). Isolated mitochondria were suspended in RIPA buffer (25 mM sucrose, 1 mM NaEGTA, 1 mM dithiothreitol, 0.1 mM PMSF, 10 mM Tris-HCl, pH 7.4, and a proteinase inhibitor mixture from Roche Applied Science). Cell lysates (0.5 mg of protein each) and mitochondrial samples (0.1 mg each) were incubated with a desired antibody (0.5–1 μg) overnight at 4 °C, followed by incubation with protein G-Sepharose beads for 1 h at room temperature or 4 °C. The beads were washed three times with IP buffer, suspended in 2× SDS loading buffer, boiled for 5 min, and used for Western blot analysis.

Mass Spectrometry—Purified porcine tubulins purchased from Cytoskeleton, Inc. (50 μg), were incubated with 30 μM AITC in 0.2 ml of PBS containing 1% acetonitrile in a glass vial for 1 h at 37 °C. A cold acetone precipitation was performed to remove unreacted AITC and salts. The protein precipitates were recovered by centrifugation, and the pellets were washed with cold 90% acetone and air-dried. The pellets were resuspended in 50 mM ammonium bicarbonate containing 10% acetonitrile, and the proteins were digested by trypsin (Sequencing Grade, Promega) at a ratio of 1:10 (w/w, trypsin/protein) at 37 °C for 2 h. The hydrolysis was stopped by the addition of formic acid to a final concentration of 2%. The samples were dried and reconstituted with 2% formic acid. The tryptic digests were analyzed by liquid chromatography, nanoelectrospray-tandem mass spectrometry (nanoLC-ESI-MS/MS) using a nanoACQUITY UPLC (Waters) coupled through a nebulization-assisted nanospray ionization source to a Q-ToF premier mass spectrometer (Waters/Micromass). MS/MS spectra were processed and transformed to the PKL file format using ProteinLynx Global Server version 2.3 (Waters/Micromass) and the default parameters of MaxEnt3 (Waters/Micromass). The PKL files were used to search a protein data base that was created using sequences obtained from GenBank™ and UniProt. Tubulin peptides modified by AITC at cysteine residues were identified by ProteinLynx Global Server and confirmed by manual inspection of the MS/MS fragment ion spectra (see supplemental material for further detail).

RT-PCR—Cells were treated with vehicle or AITC, from which total RNA was extracted using an RNeasy Mini kit (Qiagen), and 1 μg of total RNA was reverse-transcribed using SuperScript® II reverse transcriptase (Invitrogen) in a 20-μl

reaction volume. PCRs were carried out in a total volume of 25 μl, containing 1 μl of cDNA template from the above-described reaction solution, 1× PCR buffer, 1.5 mM $MgCl_2$, 0.2 mM dNTPs, 10 pmol each of the forward and reverse primers, and 1 unit of TaqDNA polymerase (Invitrogen) under the following cycle conditions: denaturation at 94 °C for 2 min, 30 cycles of 94 °C for 30 s, 58 °C for 30 s, 72 °C for 30 s, and elongation at 72 °C for 5 min. The primers included those for α-tubulin (TUBA1, forward 5′-AGTTGATTATGGCAAGAAGTCC-3′ and reverse 5′-CATCTGGTTGGCTGGCTC-3′), β-tubulin (TUBB, forward 5′-TGTTTGCTGCCTCTATCTTG-3′ and reverse 5′-CTACCCACTACCTTCTACCAT-3′), and GAPDH (forward 5′-CCAGGGCTGCTTTTAACTC-3′ and reverse 5′-GCTCCCCCCTGCAAATGA-3′).

Wright-Giemsa Staining, Immunofluorescent Staining, and DNA Staining—For Wright-Giemsa staining, cells were seeded in 10-cm dishes (1.5×10^6 cells/dish with 10 ml of medium) for 24 h and treated with solvent or AITC for 24 h. At the end of treatment, cells were harvested after trypsin treatment, washed with ice-cold PBS, and transferred to microscope slides using a Shandon Cytospin 4 from Thermo Electron Corp. Cells on the slides were dried at room temperature and stained with Wright-Giemsa solution (Sigma). After rinsing and air-drying, cover slides were affixed, and slides were analyzed by light microscopy. The percentage of mitotic figures was determined by analyzing a minimum of 150 cells in at least 20 fields per slide.

For immunofluorescent staining, cells were grown on 12-mm glass cover slides placed in 6 well plates (0.3×10^6 cells/slide with 2 ml of medium in each well) for 24 h and then exposed to solvent or AITC for 24 h. After washing once with ice-cold PBS, cells were fixed with 3.7% formaldehyde in PBS for 10 min at room temperature. Following three washes with PBS, the cells were permeabilized with wash buffer (0.1% Triton X-100 and 1% BSA in PBS) for 10 min and then treated with 10% mouse serum in PBS for 10 min. Following three more rinses with wash buffer, cells were incubated for 1 h at 37 °C with an antibody against α-tubulin. Following another three washes with wash buffer, cells were incubated with a fluorescein isothiocyanate (FITC)-conjugated secondary antibody (Santa Cruz Biotechnology) for 30 min in a dark chamber. Finally, cells were washed again with wash buffer and mounted on microscope slides with mounting medium (Molecular Probes), which contained 4′,6-diamidino-2-phenylindole (DAPI) to counterstain DNA in cells. Fluorescence microscopy was used to analyze samples.

Tubulin Polymerization Assay—The effects of AITC and BITC (the latter was used as a control) on tubulin polymerization were assessed using a tubulin polymerization assay kit (BK006) from Cytoskeleton, Inc., following the manufacturer's instruction. Briefly, bovine brain tubulin (>99% purity) at the final concentration of 3 mg/ml was incubated with solvent or AITC or BITC at 37 °C. The reaction was carried out in prewarmed microtiter plates. Absorbance readings at 340 nm were taken immediately and once every minute for 20 min, using a SPECTRAmax plate reader (Molecular Devices).

Statistical Analysis—Unpaired two-tailed Student's *t* test was used for comparison between two groups. One-way analysis of variance was used for multigroup comparison, followed by Dunnett's multiple comparison test.

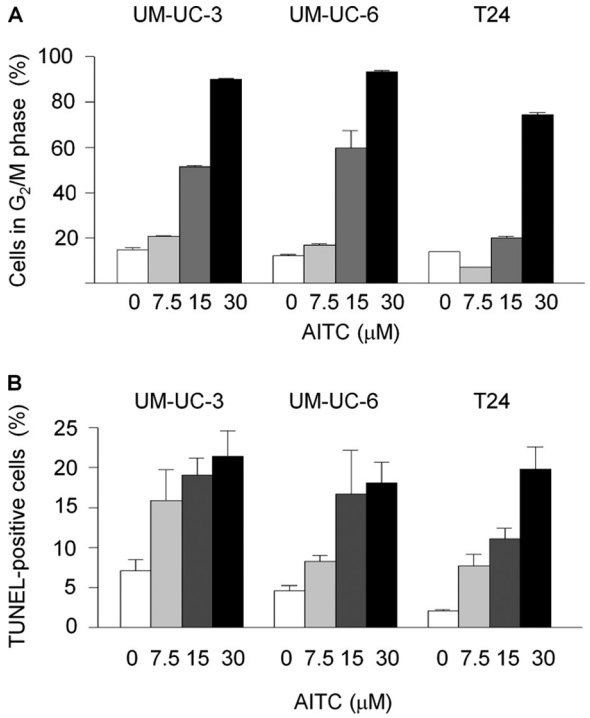

FIGURE 1. **Effect of AITC on cell cycle progression and apoptosis.** Cells were treated with vehicle or AITC for 24 h and then processed for flow cytometry analysis of cell cycle arrest (*A*, showing only G_2/M phase cells) and TUNEL-positive cells (*B*). Each value is mean ± S.D. ($n = 3$). Each value for the AITC treatment groups is significantly different from the corresponding control ($p < 0.05$).

RESULTS

AITC Causes G_2/M Arrest and Apoptosis in Human Bladder Cancer Cells—Multiple human bladder cancer cell lines were used to determine whether different cell line responds differently to AITC in terms of cell cycle arrest and apoptosis. Each cell line was treated with AITC at 0, 7.5, 15, and 30 μM for 24 h. The cells were checked either for cell cycle progression by flow cytometry or for apoptosis by a flow cytometry-based TUNEL assay. AITC caused dose-dependent and profound G_2/M arrest in all cell lines examined, with a corresponding decrease of the cell population in G_1 and S phases. Up to 90.1% of UM-UC-3 cells, up to 93.3% UM-UC-6 cells, and up to 74.5% of T24 cells existed in the G_2/M phase after AITC treatment, compared with 12.3–14.9% of control cells that were detected in these phases (Fig. 1*A*). At the same time, cells undergoing apoptosis also increased markedly after AITC treatment, as shown by an increase in both subG_1 population (see Figs. 2*A* and 3*A* for results of UM-UC-3 cells and results for UM-UC-6 cells and T24 cells not shown) and TUNEL-positive cells (Fig. 1*B*). Approximately 20% of the cells were TUNEL-positive after AITC treatment at the highest dose, compared with 2.1–7.1% in the control cells (Fig. 1*B*).

AITC Arrests Cells in Mitosis and Targets Both α- and β-Tubulin—To further understand AITC-induced cell cycle arrest, UM-UC-3 cells were treated with AITC at 15 μM for 24 h and then checked for both cell cycle arrest by flow cytometry

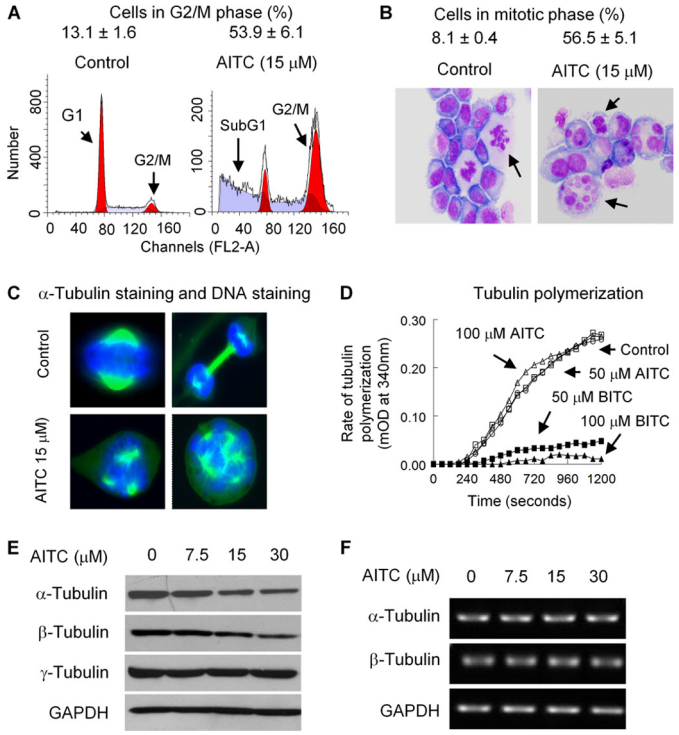

FIGURE 2. **Effect of AITC on mitosis and tubulins.** *A,* UM-UC-3 cells were treated with vehicle or AITC for 24 h and then analyzed by flow cytometry for cell cycle arrest. Each value is mean ± S.D. ($n = 3$). *B,* UM-UC-3 cells were treated with vehicle or AITC for 24 h and then subjected to Wright-Giemsa staining for counting of mitotic figures (400 cells/sample). Each value is mean ± S.D. ($n = 3$). *Arrows* point to cells in mitosis or mitotic catastrophe. *C,* UM-UC-3 cells were treated with vehicle or AITC for 24 h and then stained for microtubules with an anti-α-tubulin antibody and a fluorescein isothiocyanate (FITC)-conjugated secondary antibody (*green color*) and stained for DNA with 4′,6-diamino-2-phenylindole (*blue color*), which were subsequently visualized under a fluorescence microscope. *D,* purified bovine brain tubulin was incubated in the presence of vehicle or indicated concentrations of AITC or BITC (used as a control). Tubulin polymerization was monitored by absorbance reading at 340 nm, using an assay kit from Cytoskeleton, Inc. *E,* UM-UC-3 cells were treated with vehicle or AITC for 24 h and then measured for levels of α-, β-, and γ-tubulin by Western blotting. GAPDH was used as a loading control. Band intensity was scanned by a densitometer, and relative expression was calculated. Compared with the control, in cells treated with AITC at 30 μM, levels of α- and β-tubulin were reduced 47.1 ± 1.9 and 45.8 ± 8.4% (mean ± S.D., $n = 3$), respectively ($p < 0.05$). Representative blots are shown. *F,* UM-UC-3 cells were treated with vehicle or AITC for 24, from which total RNA was prepared for RT-PCR analysis of α- and β-tubulin, using GAPDH as a control.

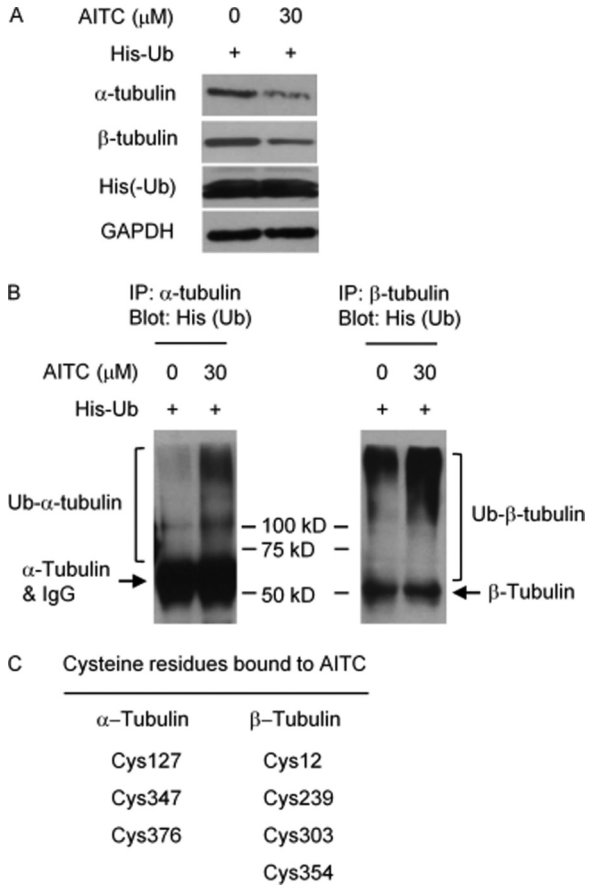

FIGURE 3. **AITC binds to tubulins and causes their ubiquitination.** UM-UC-3 cells were transfected with a His-tagged Ub expression plasmid for 24 h and then treated with vehicle or AITC for 6 h, followed by Western blot analyses of α-, β-, and His tag, with GAPDH as a control (*A*) or by IP/immunoblot analyses of ubiquitinated α-tubulin and ubiquitinated β-tubulin (*B*). Note: α-tubulin and IgG were detected simultaneously on the same blot, as both the anti-α-tubulin antibody and the anti-His tag antibody were generated in the same animal species; the anti-β-tubulin and the anti-His tag were generated in different animal species, allowing detection of β-tubulin without interference by IgG. *C,* purified porcine tubulins were incubated with AITC at 30 μM for 1 h at 37 °C and then precipitated with acetone, followed by the identification of AITC-bound cysteine residues by mass spectrometry (see supplemental material for detail).

and mitotic figures (both mitotic cells and cells with multiple micronuclei) after Wright-Giemsa staining. 53.9% of AITC-treated cells were arrested in G_2/M phase *versus* 13.1% in control cells (Fig. 2*A*), which were similar to that shown in Fig. 1*A*. Interestingly, Wright-Giemsa staining revealed that 56.5% of AITC-treated cells were in the mitotic phase *versus* 8.1% in control cells (Fig. 2*B*). Thus, AITC caused predominantly if not entirely mitotic arrest, rather than G_2 phase arrest. It is also of note that a significant population of AITC-treated cells showed multiple micronuclei (Fig. 2*B*), indicative of mitotic catastrophe. Simultaneous immunostaining of α-tubulin (Fig. 2*C, green color*) and DNA staining with DAPI (*blue color*) showed control cells undergoing typical mitosis and cell division (bipolar mitotic spindle and separation of sister chromosomes), whereas AITC-treated cells exhibited aberrant and multipolar mitotic spindle and lack of separation of sister chromosomes, reminiscent of the effects of vinblastine, which is a microtubule depolymerizer, and taxol, which is a microtubule stabilizer (9). However, AITC does not affect tubulin polymerization, as AITC at 50 and 100 μM had no effect on the rate of tubulin polymerization in an *in vitro* assay, whereas another isothiocyanate (BITC, used as a control) at the same concentrations almost completely inhibited tubulin polymerization (Fig. 2*D*). Further experiments showed that AITC significantly down-regulated both α- and β-tubulin, but not γ-tubulin (Fig. 2*E*), suggesting that α- and β-tubulin may be key AITC targets for mitotic arrest. Interestingly, AITC had no effect on the transcripts of either α-tubulin gene or β-tubulin gene (Fig. 2*F*), indicating that AITC likely destabilized the proteins coded by these genes. Indeed, although treatment of UM-UC-3 cells with AITC (30 μM, 6 h) decreased the levels of both α- and β-tubulin (Fig. 3*A*), there was a marked increase in the levels of ubiquitinated α-tubulin and ubiquitinated β-tubulin (Fig. 3*B*), suggesting that AITC promoted the degradation of the tubulins via the ubiquitin (Ub)-proteasome pathway. Similar results were obtained in cells treated with AITC at 30 μM for 3 h (data not

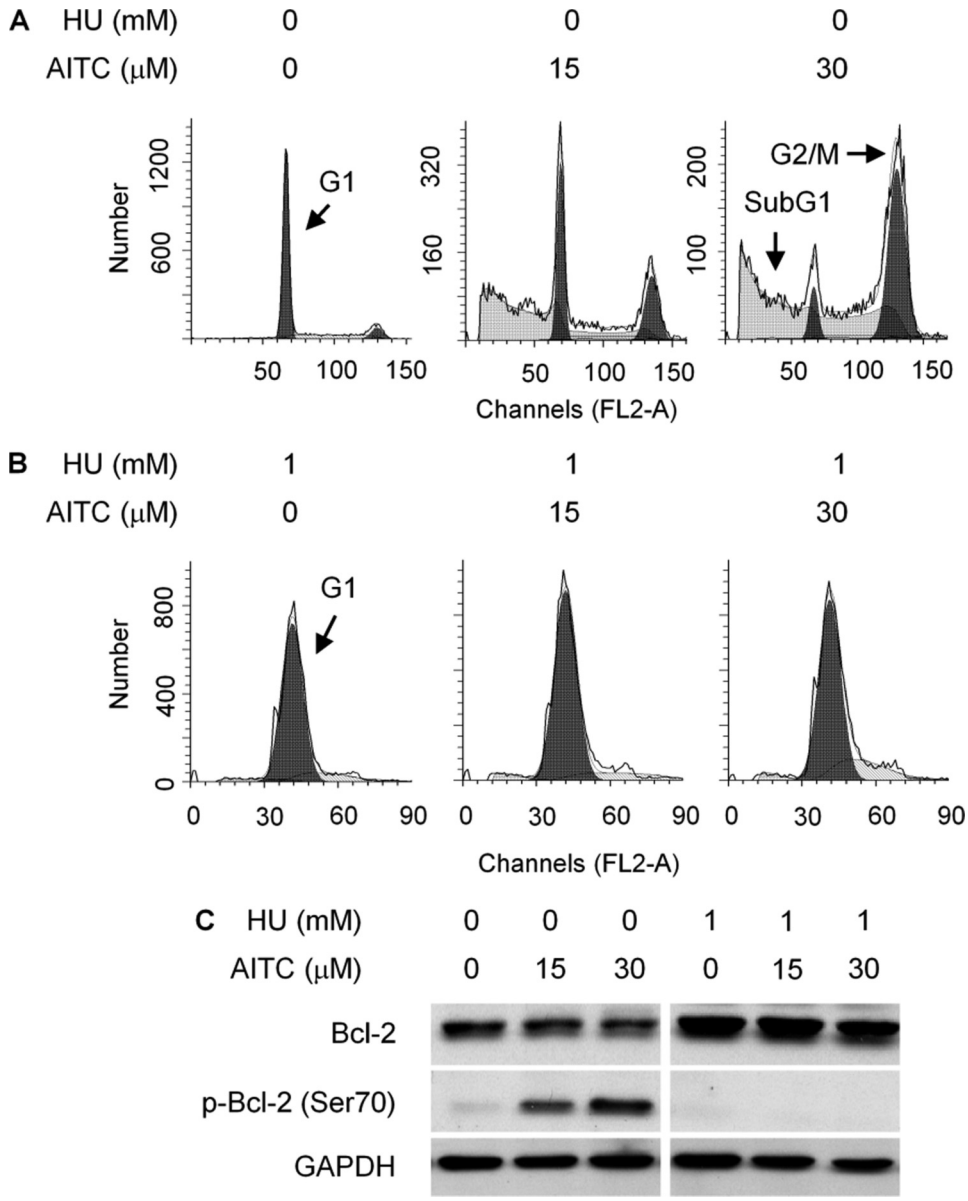

FIGURE 4. **Relationship between cell cycle arrest and Bcl-2 phosphorylation caused by AITC.** *A* and *B,* UM-UC-3 cells were pretreated with or without HU for 16 h and then treated with vehicle or AITC for 24 h in the presence or absence of HU, followed by flow cytometry analysis of cell cycle progression. *C,* UM-UC-3 cells were pretreated with or without HU for 16 h and then treated with vehicle or AITC for 24 h in the presence or absence of HU, followed by Western blotting of Bcl-2 and p-Bcl-2. The anti-p-Bcl-2 antibody detected specifically Ser(P)-70. GAPDH is a loading control.

shown). It is of note that the cells in the above experiments were transfected with a His-tagged Ub expression plasmid for 24 h before AITC treatment; in the absence of ectopic Ub expression, neither Ub-α-tubulin nor Ub-β-tubulin was detectable (data not shown). Moreover, incubation of purified porcine α-/β-tubulins with 30 μM AITC for 1 h at 37 °C resulted in binding of AITC to specific cysteine (Cys) residues, including Cys-127, Cys-347, and Cys-376 of α-tubulin, and Cys-12, Cys-239, Cys-303, and Cys-354 of β-tubulin, as shown by mass spectrometry analysis of trypsin-digested peptide fragments (Fig. 3*C* and supplemental Fig. S3). However, AITC binding to the cysteine residues was reversible, as the result described above was obtained after trypsin digestion of the AITC-treated tubulins for 2 h at 37 °C, whereas no cysteine modification by AITC could be detected after overnight incubation of the AITC-treated tubulins with trypsin (data not shown). The reversible nature of AITC binding to tubulin cysteines is consistent with our inability to detect AITC binding to cysteine residues of tubulins in UM-UC-3 cells, where the cells were treated with AITC at 30 μM for 3 h, from which α-/β-tubulins were isolated by immunoprecipitation and/or gel electrophoresis before they were subjected to trypsin digestion and mass spectrometry analysis. Nevertheless, the AITC-binding cysteine residues of the porcine tubulins, as described above, are also present in human α-/β-tubulins.

AITC-induced Cell Death Depends on Mitotic Arrest and Is Associated with Phosphorylation of JNK and Bcl-2—To further characterize mitotic arrest induced by AITC, UM-UC-3 cells were pretreated with or without 1 mM HU for 16 h and then treated with AITC at 15 and 30 μM for 24 h in the presence or

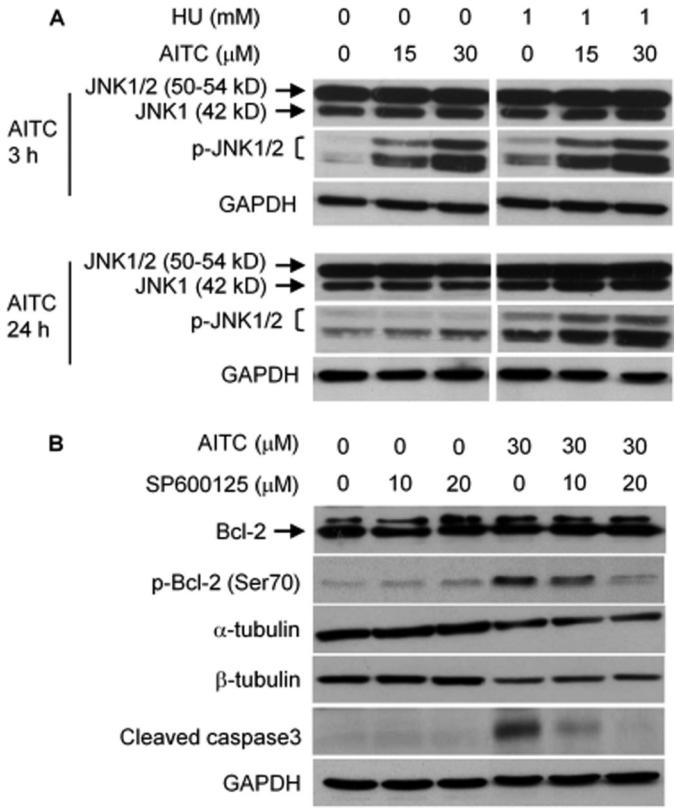

FIGURE 5. **JNK activation by AITC and its role in Bcl-2 phosphorylation.** *A,* UM-UC-3 cells were pretreated with or without HU for 16 h and then treated with vehicle or AITC for 3 or 24 h in the presence or absence of HU, followed by Western blotting of JNK and p-JNK (Thr-183/Tyr-185). *B,* UM-UC-3 cells were pretreated with SP600125 (a JNK inhibitor) for 1 h and then co-treated with AITC and SP600125 for 24 h, followed by Western blotting of Bcl-2, p-Bcl-2 (Ser-70), and several other proteins. GAPDH is a loading control.

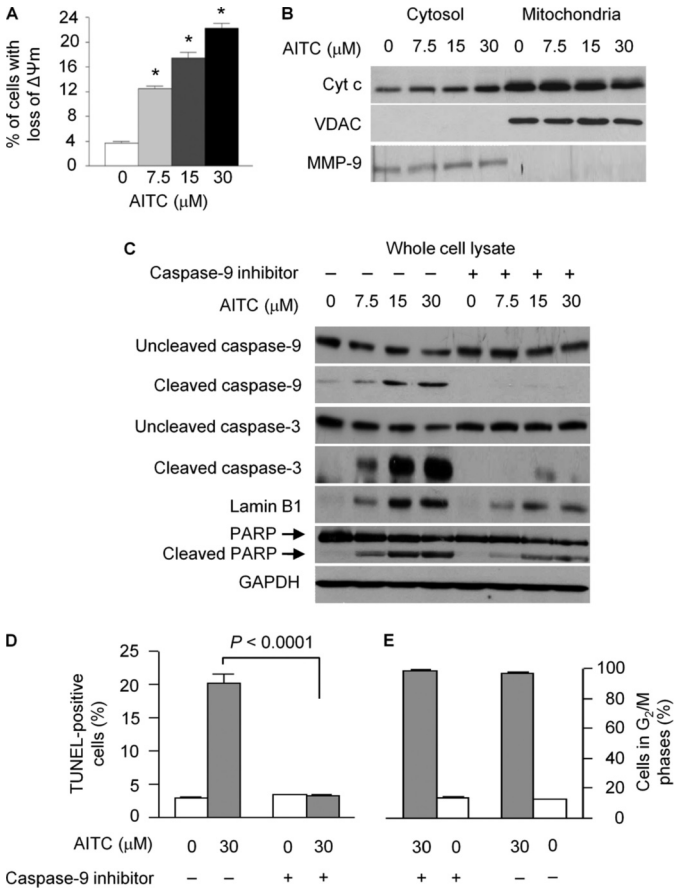

FIGURE 6. **Effect of AITC on mitochondrion-mediated apoptosis.** *A,* UM-UC-3 cells were treated with vehicle or AITC for 24 h, then labeled with rhodamine 123, and finally measured for loss of mitochondrial transmembrane potential ($\Delta\Psi m$) by flow cytometry. Each value is mean ± S.D. ($n = 3$); *, $p < 0.0001$, compared with the control. *B,* UM-UC-3 cells were treated with vehicle or AITC for 24 h, from which cytosol and mitochondria were prepared and measured for Cyt *c* by Western blotting. Voltage-dependent anion channel (*VDAC*, a mitochondrial protein) was measured to rule out the presence of mitochondria in the cytosolic samples. MMP-9 (a cytosolic protein) was measured to rule out the presence of cytosolic materials in the mitochondrial samples. *C,* UM-UC-3 cells were pretreated with vehicle or a caspase 9 inhibitor (Z-LEHD-FMK, 20 μM) for 1 h and then exposed to AITC in the presence or absence of Z-LEHD-FMK (20 μM) for 24 h. Cell lysates were analyzed by Western blotting for various proteins. *D* and *E,* UM-UC-3 cells were treated with vehicle or AITC in the presence or absence of Z-LEHD-FMK (20 μM) for 24 h and then analyzed for the presence of apoptotic cells (TUNEL-positive cells) and for cell cycle arrest by flow cytometry. Each value is mean ± S.D. ($n = 3$).

absence of HU. HU is a DNA replication inhibitor and arrests cells in G_1 phase. Indeed, HU completely arrested UM-UC-3 cells in G_1 phase and prevented AITC from arresting cells in mitosis, as measured by flow cytometry (Fig. 4, *A* and *B*). More interestingly, HU also prevented AITC from causing cell death, as subG_1 population, which formed after AITC treatment (Fig. 4*A*), was no longer detected in cells co-treated with HU and AITC (Fig. 4*B*). Moreover, AITC stimulated Bcl-2 phosphorylation at Ser-70, although not at Ser-87 (antibodies specific for phosphorylation at each site were used), while not affecting total Bcl-2 expression (Figs. 4*C* and 7*C*). A subsequent experiment showed that AITC-induced Bcl-2 phosphorylation occurred exclusively in the mitochondria (Fig. 7*C*). However, HU completely blocked AITC-induced Bcl-2 phosphorylation (Fig. 4*C*), indicating that mitotic arrest is a prerequisite for AITC to induce Bcl-2 phosphorylation. Bcl-2 is a major anti-apoptotic protein, and Bcl-2 phosphorylation is well known to modulate its anti-apoptotic activity. Our finding that Bcl-2 phosphorylation was closely associated with the formation of subG_1 cells after AITC treatment suggested that Bcl-2 phosphorylation might be key to AITC-induced cell death. Subsequent experiments showed that JNK was responsible for AITC-induced Bcl-2 phosphorylation. UM-UC-3 cells express both JNK1 (42 and 50 kDa) and JNK2 (54 kDa), but not JNK3, as detected by Western blotting using antibodies specific for each isoform (see supplemental Fig. S1). The results shown in Fig. 5*A* were obtained using antibodies detecting all JNKs or JNKs that are phosphorylated at Thr-183/Tyr-185. Two Western blot bands of JNK and p-JNK were detected, corresponding to total and phosphorylated JNK1 and JNK2 (Fig. 5*A* and supplemental Fig. S1). Cells were pretreated with solvent or HU for 16 h and then treated with AITC for 3 or 24 h with or without HU. In cells treated with AITC alone, although it had no effect on the expression levels of total JNK1 and JNK2, it caused rapid phosphorylation at Thr-183/Tyr-185 of JNK1 and probably JNK2 (the 50–54-kDa band likely represents both p-JNK1 and p-JNK2), as 3-h AITC treatment caused marked increase in p-JNK1/2; the effect was much attenuated after 24 h AITC treatment (Fig. 5*A*). Moreover, a specific JNK inhibitor (SP600125) inhibited AITC-induced Bcl-2 phosphorylation (Fig. 5*B*), and Bcl-2 Ser-70 is a known JNK phosphorylation site (10). Another JNK inhibitor XI, BI-87G3, which is structurally

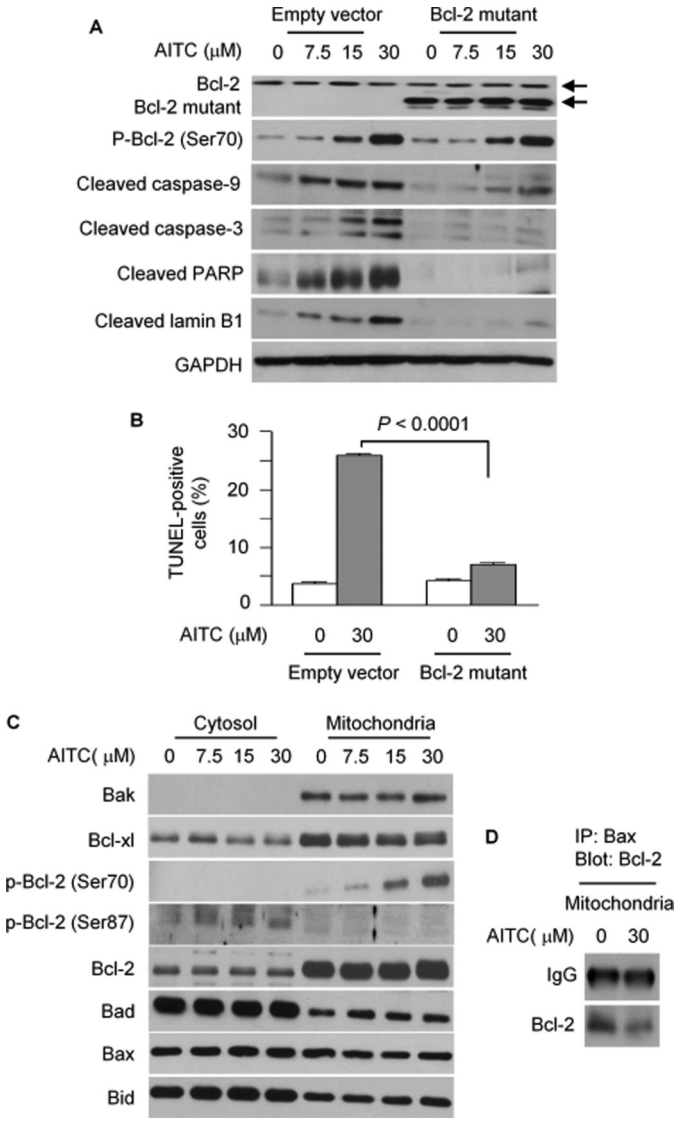

FIGURE 7. **Role of Bcl-2 phosphorylation in AITC-induced apoptosis.** *A,* UM-UC-3 cells were transfected in an equal amount of DNA with either the empty vector or the Bcl-2 loop deletion mutant for 24 h and then exposed to vehicle or AITC for 24 h, followed by Western blotting of various proteins. *B,* UM-UC-3 cells were treated as described in *A* and then measured by flow cytometry for TUNEL-positive cells. Each value is mean ± S.D. ($n = 3$). *C,* UM-UC-3 cells were treated with vehicle or AITC for 24 h, from which mitochondria and cytosol were prepared and analyzed by Western blotting for various proteins. Bcl-2 phosphorylation at Ser-70 and Ser-87 were also measured. *D,* UM-UC-3 cells were treated with solvent or AITC for 24 h, from which mitochondria were purified and subjected to immunoprecipitation (*IP*) with anti-Bax and Western blotting (using 4–15% gradient gel) with anti-Bcl-2.

different from SP600125, also inhibited AITC-induced Bcl-2 phosphorylation in UM-UC-3 cells (supplemental Fig. S2). These results show that AITC causes Bcl-2 phosphorylation at Ser-70 via JNK activation. SP600125 also inhibited AITC-induced caspase 3 activation (Fig. 5*B*), providing further evidence that JNK-mediated Bcl-2 phosphorylation is important in AITC-induced cell death. However, JNK inhibition by SP600125 had no effect on down-regulation of α-/β-tubulins by AITC (Fig. 5*B*). Interestingly, in cells treated with both AITC and HU, there was a sustained JNK1/2 phosphorylation and a slight increase in JNK1 expression levels (Fig. 5*A*) but no Bcl-2 phosphorylation (Fig. 4*B*), hinting that AITC-activated JNK is not able to phosphorylate Bcl-2 unless cells are arrested in mitosis.

AITC Activates Mitochondrion-mediated Apoptosis—Treatment of UM-UC-3 cells with AITC at 7.5–30 μM caused a dose-dependent and up to 6-fold loss of ΔΨm (mitochondrial transmembrane potential) (Fig. 6*A*), cytoplasmic accumulation of Cyt *c* and corresponding decrease of mitochondrial Cyt *c* (Fig. 6*B*), cleavage and/or activation of caspase-9, caspase-3, lamin B1, and PARP (Fig. 6*C*), and 7.2-fold increase in TUNEL-positive cells (Fig. 6*D*), clearly showing strong activation of the mitochondrion-mediated apoptosis by AITC. Both PARP and lamin B1 are known substrates of caspase-3. Moreover, a caspase-9 inhibitor (Z-LEHD-FMK, 20 μM) almost completely blocked AITC-induced cleavage of both caspase-3 and caspase-9 and the cleavage of PARP and lamin B1 (Fig. 6*C*), and it also prevented AITC from inducing TUNEL-positive cells (Fig. 6*D*), but it had no effect on AITC-induced cell cycle arrest (Fig. 6*E*). These results indicate that AITC caused the cells to die through mitochondrion-mediated apoptosis. The finding is consistent with the current understanding that cell death by mitotic catastrophe involves activation of the mitochondrial apoptotic pathway (11). It is also worth noting that, in the cytoplasmic fractions, we also observed marked decrease in both α- and β-tubulin levels after AITC treatment (result not shown).

Bcl-2 Is Key to Apoptosis Activation by AITC—As described above, Bcl-2 phosphorylation was closely associated with mitotic arrest and cell death after AITC treatment, and AITC-induced Bcl-2 phosphorylation occurred exclusively in the mitochondria (Fig. 7*C*); AITC strongly activated the mitochondrial apoptosis pathway, and a caspase-9 inhibitor completely blocked AITC-induced apoptosis (Fig. 6). In light of these findings, we asked if a Bcl-2 mutant lacking phosphorylation would inhibit AITC-induced cell death. We used a loop deletion Bcl-2 mutant with amino acid residues 32–80 removed. The loop domain of Bcl-2 contains Ser-70 and several other phosphorylation sites, and deletion of this domain was previously shown to block apoptosis induction by Taxol and other agents in certain cell lines (12, 13). UM-UC-3 cells were transfected with either the empty vector (pSFFV-neo) or the Bcl-2 mutant (pSFFV-HA-hBcl-2Δ), and 24 h after the transfection the cells were treated with either vehicle or AITC at 7.5–30 μM for 24 h. The Bcl-2 mutant was expressed ~3-fold higher than the endogenous Bcl-2 (Fig. 7*A*), and the expression levels of neither the endogenous Bcl-2 nor the mutant were influenced by AITC (Fig. 7*A*). The mutant did not affect AITC-induced phosphorylation of endogenous Bcl-2 (Fig. 7*A*). However, expression of the Bcl-2 mutant markedly attenuated the cleavage and/or activation of caspase-9, caspase-3, PARP, and lamin B1 (Fig. 7*A*). Moreover, induction of TUNEL-positive cells by AITC (30 μM, 24 h) was 73% lower in UM-UC-3 cells transfected with the Bcl-2 mutant than in cells transfected with the empty vector (Fig. 7*B*). It is possible that the inhibition of apoptosis might be even more complete, if the mutant could be expressed to higher levels.

We also examined the effect of AITC on several other Bcl-2 family members that are known to play a role in apoptosis, including Bak, Bcl-xl, Bad, Bax, and Bid. UM-UC-3 cells were treated with vehicle or AITC for 24 h, followed by Western

blotting of these proteins and Bcl-2. Except for Bak, which was detected only in the mitochondria, other proteins were detected in both the mitochondria and cytosol. However, AITC had no effect on their expression levels in either mitochondria or cytoplasm, except for stimulating Bcl-2 phosphorylation at Ser-70 in the mitochondria (Fig. 7*C*). Nevertheless, in UM-UC-3 cells treated with AITC for 24 h, Bcl-2 association with Bax in the mitochondria was disrupted, as measured by IP of purified mitochondrial lysates with anti-Bax and immunoblot with anti-Bcl-2 (Fig. 7*D*).

DISCUSSION

AITC causes G_2/M arrest in a wide variety of human cancer cell lines, such as the three bladder cancer lines shown in this study, cervical cancer HeLa cells (14), colorectal cancer HT29 cells (15), and prostate cancer PC-3 cells and LNCaP cells (16). Using UM-UC-3 cell as a model and employing both flow cytometry and Wright-Giemsa staining, we have demonstrated that AITC arrests cancer cells in M phase, rather than G_2 phase. Mitotic block was previously detected in AITC-treated HT29 cells by counting metaphase cells using transmission electron microscopy, but the study did not address the extent of mitotic arrest or whether AITC arrested HT29 cells in both G_2 phase and M phase (15). Our results also indicate that AITC is a highly effective mitosis-blocking agent, as a single AITC treatment led up to more than 90% of the UM-UC-3 cells arrested. Unlike taxol and vinblastine, which are widely used in the clinic for cancer treatment and block mitosis by either stabilizing or destabilizing microtubule polymer, our study shows that AITC does not affect microtubule stability. Rather, AITC down-regulates both α- and β-tubulin, albeit not γ-tubulin. Thus, AITC is a new class of mitotic blocker. However, the ability of AITC to down-regulate α- and β-tubulin appears to be shared by other isothiocyanates, as Chung and co-workers (17, 18) recently showed that BITC, phenethyl isothiocyanate, and sulforaphane also down-regulated both tubulins in human lung cancer A549 cells and several other cell lines. These previous studies also showed that the isothiocyanates did not affect the transcription of the tubulin genes but stimulated proteasome-mediated degradation of the proteins. Indeed, this study showed that AITC had no effect on the transcript levels of both α- and β-tubulin but stimulated ubiquitination of both tubulins, indicating that AITC stimulates proteasome-mediated degradation of the tubulins. We further showed that AITC directly bound to multiple cysteine residues of both α-tubulin (Cys-127, Cys-347, and Cys-376) and β-tubulin (Cys-12, Cys-239, Cys-303, and Cys-354), but the binding was reversible. This is consistent with the knowledge that the –N=C=S group of AITC is electrophilic and readily reacts with cysteine thiols, but the reaction is reversible (1). Although it remains to be determined if AITC binding to the cysteine residues or a specific cysteine residue of the tubulins is responsible for increased ubiquitination, most of the β-tubulin cysteine residues targeted by AITC have also been shown to be targeted by a number of antitumor agents, including Cys-12 by bis(4-fluorobenzyl)trisulfide and arsenic (19, 20), Cys-239 by 2-fluoro-1-methoxy-4-pentafluorophenylsulfonamidobenzene (21), and Cys-239 and Cys-354 by colchicine and colchicinoids (22, 23). Moreover, mutagenesis of Cys-12 or Cys-354 in β-tubulin was either lethal or significantly affected the structure and function of the tubulin in *Saccharomyces cerevisiae* (24).

Previous studies showed that cell cycle arrest in AITC-treated cells was always accompanied by apoptosis. This is also true for the three bladder cancer cell lines examined in this study; all of them showed cell cycle arrest, formation of subG_1 cells, and TUNEL-positive cells in response to AITC. Using UM-UC-3 cells as a model, and preventing AITC from causing mitotic arrest by first arresting UM-UC-3 cells in G_1 phase with HU, we found that AITC was no longer able to cause cell death. Moreover, although significant Bcl-2 phosphorylation was always associated with AITC-induced cell cycle arrest in all the bladder cancer cell lines examined in our study, such a change was no longer detected in cells pretreated with HU, followed by AITC. Thus, AITC-induced Bcl-2 phosphorylation depends on mitotic arrest. We further showed that AITC-induced Bcl-2 phosphorylation was associated with JNK activation (JNK1 and probably JNK2), and JNK inhibition prevented AITC from inducing Bcl-2 phosphorylation, indicating that AITC induces Bcl-2 phosphorylation by activating JNK. How AITC activates JNK remains unknown at this time. It is worth noting that both Taxol and vinblastine, both of which arrest cells in mitosis, also cause Bcl-2 phosphorylation (25, 26). Therefore, it seems likely that Bcl-2 phosphorylation occurs due to mitotic arrest, rather than an AITC-specific effect. Because Bcl-2 is a well known anti-apoptotic protein and Bcl-2 phosphorylation is known to affect its activity, we asked if Bcl-2 phosphorylation was involved in AITC-induced cell death. In UM-UC-3 cells, AITC-induced Bcl-2 phosphorylation occurred exclusively in the mitochondria. AITC did not modulate other Bcl-2 family proteins, including Bak, Bcl-xl, Bad, Bax, and Bid, but disrupted the association of Bcl-2 with Bax. AITC also activated the mitochondrion-mediated apoptosis, including the loss of mitochondrial transmembrane potential, cytoplasmic accumulation of Cyt *c*, activation of caspase-9, activation of caspase-3, and cleavage of PARP and lamin B1. Both PARP and lamin B1 are known substrates of caspase-3. This apoptotic pathway is essential for AITC to kill UM-UC-3 cells, as a caspase-9 inhibitor not only blocked AITC from activating both caspase-9 and caspase-3 and from causing cleavage of both lamin B1 and PARP but also blocked AITC from inducing the TUNEL-positive cells. Moreover, in cells transiently transfected with a Bcl-2 mutant that lacks the phosphorylation site, although the expression and AITC-induced phosphorylation of the endogenous Bcl-2 were not affected by the Bcl-2 mutant, AITC-induced apoptosis was markedly inhibited by the mutant, including inhibition of the activation of both caspase-9 and caspase-3, inhibition of the cleavage of both PARP and lamin B1, and inhibition of the formation of TUNEL-positive cells. Although the whole loop domain of Bcl-2 was deleted in this mutant, removing both the JNK phosphorylation site (Ser-70) and several other phosphorylation sites, it is of note that microtubule-targeting drugs typically induce Bcl-2 phosphorylation at Ser-70 and Ser-87 (27–29), but we showed that AITC did not stimulate Bcl-2 phosphorylation at Ser-87. Taken together, we conclude that Bcl-2 phosphorylation at Ser-70 bridges mitotic arrest to apoptosis in response to AITC.

In summary, our study shows that AITC binds to cysteine residues of α- and β-tubulin, promotes their ubiquitination and degradation, and arrests cancer cells exclusively in mitosis, which leads to cell death by mitotic catastrophe through the mitochondrion-mediated apoptosis. Bcl-2 phosphorylation at Ser-70, which is caused by JNK activation, is the molecular linker between mitotic arrest and apoptosis in AITC-treated cells. Moreover, AITC is a new class of mitosis blocker, as its mechanism of action differs from that of taxol and vinblastine that modulate tubulin polymer stability. Although these novel findings have been made in human bladder cancer cells and are important for further development of this agent against bladder cancer, they may not be specific to bladder cancer cells. Experiments to verify and extend the intriguing anticancer mechanisms of AITC in cancer cells of other tissue origins are warranted.

Acknowledgments—We greatly appreciate the gift of Bcl-2 mutant plasmid from Dr. Craig B. Thompson (University of Pennsylvania) and the gift of pMT107-His-Ub plasmid from Dr. Xinjiang Wang (Roswell Park Cancer Institute).

REFERENCES

1. Zhang, Y. (2010) *Mol. Nutr. Food Res.* **54,** 127–135
2. Bhattacharya, A., Tang, L., Li, Y., Geng, F., Paonessa, J. D., Chen, S. C., Wong, M. K., and Zhang, Y. (2010) *Carcinogenesis* **31,** 281–286
3. Bhattacharya, A., Li, Y., Wade, K. L., Paonessa, J. D., Fahey, J. W., and Zhang, Y. (2010) *Carcinogenesis* **31,** 2105–2110
4. Michaud, D. S., Spiegelman, D., Clinton, S. K., Rimm, E. B., Willett, W. C., and Giovannucci, E. L. (1999) *J. Natl. Cancer Inst.* **91,** 605–613
5. Tang, L., Zirpoli, G. R., Guru, K., Moysich, K. B., Zhang, Y., Ambrosone, C. B., and McCann, S. E. (2008) *Cancer Epidemiol. Biomarkers Prev.* **17,** 938–944
6. Tang, L., and Zhang, Y. (2004) *J. Nutr.* **134,** 2004–2010
7. Tang, L., Li, G., Song, L., and Zhang, Y. (2006) *Anticancer Drugs* **17,** 297–305
8. Yu, S. W., Wang, H., Poitras, M. F., Coombs, C., Bowers, W. J., Federoff, H. J., Poirier, G. G., Dawson, T. M., and Dawson, V. L. (2002) *Science* **297,** 259–263
9. Jo, H., Loison, F., Hattori, H., Silberstein, L. E., Yu, H., and Luo, H. R. (2010) *PLoS One* **5,** e10318
10. Deng, X., Xiao, L., Lang, W., Gao, F., Ruvolo, P., and May, W. S., Jr. (2001) *J. Biol. Chem.* **276,** 23681–23688
11. Castedo, M., Perfettini, J. L., Roumier, T., Andreau, K., Medema, R., and Kroemer, G. (2004) *Oncogene* **23,** 2825–2837
12. Chang, B. S., Minn, A. J., Muchmore, S. W., Fesik, S. W., and Thompson, C. B. (1997) *EMBO J.* **16,** 968–977
13. Srivastava, R. K., Mi, Q. S., Hardwick, J. M., and Longo, D. L. (1999) *Proc. Natl. Acad. Sci. U.S.A.* **96,** 3775–3780
14. Hasegawa, T., Nishino, H., and Iwashima, A. (1993) *Anticancer Drugs* **4,** 273–279
15. Smith, T. K., Lund, E. K., Parker, M. L., Clarke, R. G., and Johnson, I. T. (2004) *Carcinogenesis* **25,** 1409–1415
16. Xiao, D., Srivastava, S. K., Lew, K. L., Zeng, Y., Hershberger, P., Johnson, C. S., Trump, D. L., and Singh, S. V. (2003) *Carcinogenesis* **24,** 891–897
17. Mi, L., Xiao, Z., Hood, B. L., Dakshanamurthy, S., Wang, X., Govind, S., Conrads, T. P., Veenstra, T. D., and Chung, F. L. (2008) *J. Biol. Chem.* **283,** 22136–22146
18. Mi, L., Gan, N., Cheema, A., Dakshanamurthy, S., Wang, X., Yang, D. C., and Chung, F. L. (2009) *J. Biol. Chem.* **284,** 17039–17051
19. Xu, W., Xi, B., Wu, J., An, H., Zhu, J., Abassi, Y., Feinstein, S. C., Gaylord, M., Geng, B., Yan, H., Fan, W., Sui, M., Wang, X., and Xu, X. (2009) *Mol. Cancer Ther.* **8,** 3318–3330
20. Zhang, X., Yang, F., Shim, J. Y., Kirk, K. L., Anderson, D. E., and Chen, X. (2007) *Cancer Lett.* **255,** 95–106
21. Shan, B., Medina, J. C., Santha, E., Frankmoelle, W. P., Chou, T. C., Learned, R. M., Narbut, M. R., Stott, D., Wu, P., Jaen, J. C., Rosen, T., Timmermans, P. B., and Beckmann, H. (1999) *Proc. Natl. Acad. Sci. U.S.A.* **96,** 5686–5691
22. Bai, R., Pei, X. F., Boyé, O., Getahun, Z., Grover, S., Bekisz, J., Nguyen, N. Y., Brossi, A., and Hamel, E. (1996) *J. Biol. Chem.* **271,** 12639–12645
23. Bai, R., Covell, D. G., Pei, X. F., Ewell, J. B., Nguyen, N. Y., Brossi, A., and Hamel, E. (2000) *J. Biol. Chem.* **275,** 40443–40452
24. Gupta, M. L., Jr., Bode, C. J., Dougherty, C. A., Marquez, R. T., and Himes, R. H. (2001) *Cell Motil. Cytoskeleton* **49,** 67–77
25. Haldar, S., Chintapalli, J., and Croce, C. M. (1996) *Cancer Res.* **56,** 1253–1255
26. Fan, M., Goodwin, M., Vu, T., Brantley-Finley, C., Gaarde, W. A., and Chambers, T. C. (2000) *J. Biol. Chem.* **275,** 29980–29985
27. Yamamoto, K., Ichijo, H., and Korsmeyer, S. J. (1999) *Mol. Cell. Biol.* **19,** 8469–8478
28. Haldar, S., Basu, A., and Croce, C. M. (1998) *Cancer Res.* **58,** 1609–1615
29. Basu, A., and Haldar, S. (1998) *Int. J. Oncol.* **13,** 659–664